Joint Laboratory of Solid-State NMR IMC AS CZ and JHIPC AS CZ

Institute of Macromolecular Chemistry AS CR
Heyrovsky Sqr. 2
162 06 Praha 6
Czech Republ.

(2)

Dynamics of multicomponent polymer systems:

^{1}H-^{13}C wide-line separation experiments and spin diffusion

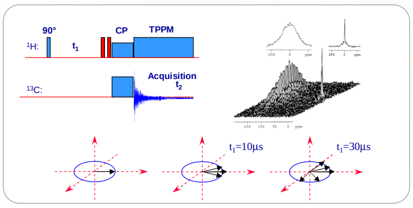

Separation experiments

Hans W. Spiess
*1933

2D ^{1}H-^{13}C WISE

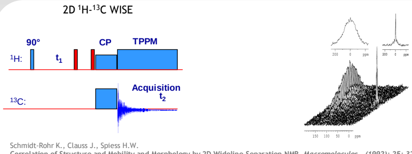

Schmidt-Rohr K., Clauss J., Spiess H.W.
Correlation of Structure and Mobility and Morphology by 2D Wideline-Separation NMR, *Macromolecules*. (1992); 25: 3273.

RG Griffin

2D ^{1}H-^{15}N SLF NMR

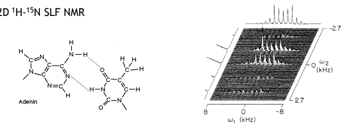

Griffin R.G.
Measurement of Heteronuclear Bond Distances in Polycrystalline Solids by Solid-State NMR, *J.Am.Chem.Soc.* (1987); 109: 4163.

Principles of separation of ^{1}H-^{1}H dipolar spectra

Strong dipolar interactions ^{1}H-^{1}H (30-50 kHz)
^{1}H chemical shift is neglected (2 kHz)
Cosine data are recorded

2D ^{1}H-^{13}C WISE

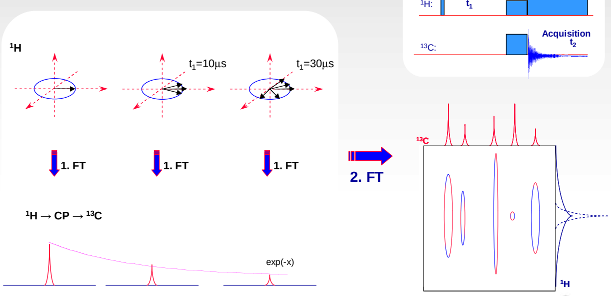

Schmidt-Rohr K., Clauss J., Spiess H.W.
Correlation of Structure and Mobility and Morphology by 2D Wideline-Separation NMR, *Macromolecules*. (1992); 25: 3273.

Principles of separation of ^{1}H-^{1}H dipolar spectra

Polycarbonate-PEO

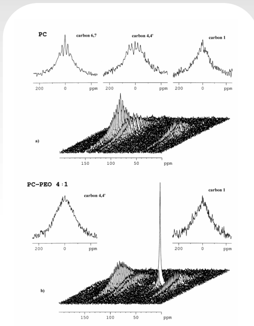

2D ^{1}H-^{13}C WISE

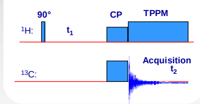

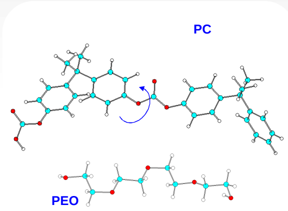

Principles of separation of ^{1}H-^{1}H dipolar spectra

Polyimide-Polydimethylsiloxane

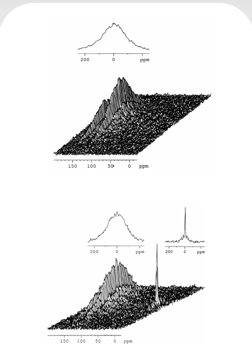

2D ^{1}H-^{13}C WISE

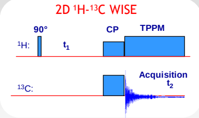

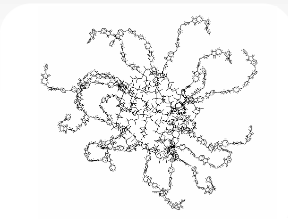

Spin-diffusion in WISE dipolar spectra

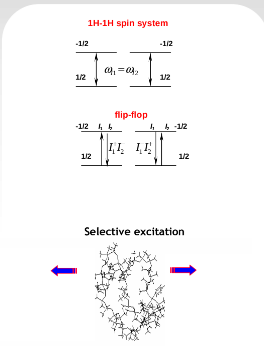

2D ^{1}H-^{13}C WISE

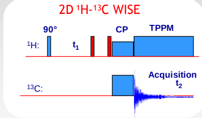

Polyimide-Polydimethylsiloxane

Without SD
Limited SD
Short 0,5 ms
Full SD
Long 40,5 ms

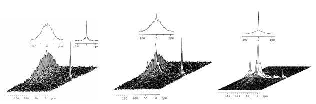

^1H-^1H spin exchange (diffusion)

Selection and transfer of magnetization

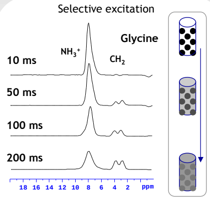

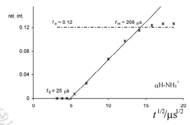

Spin diffusion: $$\frac{\partial M(r,t)}{\partial t} = \frac{\partial}{\partial x}\left[D\frac{\partial}{\partial x}M(r,t)\right]+\frac{\partial}{\partial y}\left[D\frac{\partial}{\partial y}M(r,t)\right]+\frac{\partial}{\partial z}\left[D\frac{\partial}{\partial z}M(r,t)\right]$$

Size of dispersed component A in matrix B : $$d_A = 2\frac{\varepsilon}{f_B}\left(\frac{1}{\pi}Dt_m^s\right)^{1/2}$$

Relations of spin-diffusion coefficients and segmental dynamics:

$$D_{rig} = \frac{1}{12}\sqrt{\frac{\pi}{2\ln 2}}\langle r^2\rangle\Delta\nu_{1/2} \qquad D_{mob} = \frac{1}{6}\langle r^2\rangle[\alpha\Delta\nu_{1/2}]^{1/2}$$

$$D_{mob} = 8.2\times10^{-6}T_2^{-1}+0.007 \qquad D_{mob} = 4.4\times10^{-5}T_2^{-1}+0.26$$

^1H-^1H spin exchange (diffusion)

Selection and transfer of magnetization

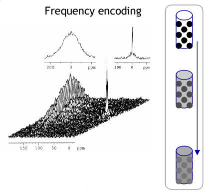

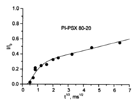

Spin diffusion: $$\frac{\partial M(r,t)}{\partial t} = \frac{\partial}{\partial x}\left[D\frac{\partial}{\partial x}M(r,t)\right]+\frac{\partial}{\partial y}\left[D\frac{\partial}{\partial y}M(r,t)\right]+\frac{\partial}{\partial z}\left[D\frac{\partial}{\partial z}M(r,t)\right]$$

Size of dispersed component A in matrix B : $$d_A = 2\frac{\varepsilon}{f_B}\left(\frac{1}{\pi}Dt_m^s\right)^{1/2}$$

Relations of spin-diffusion coefficients and segmental dynamics:

$$D_{rig} = \frac{1}{12}\sqrt{\frac{\pi}{2\ln 2}}\langle r^2\rangle\Delta\nu_{1/2} \qquad D_{mob} = \frac{1}{6}\langle r^2\rangle[\alpha\Delta\nu_{1/2}]^{1/2}$$

$$D_{mob} = 8.2\times10^{-6}T_2^{-1}+0.007 \qquad D_{mob} = 4.4\times10^{-5}T_2^{-1}+0.26$$

$$D = 0{,}05 - 0{,}8\,nm^2\,ms^{-1}$$

^1H-^1H spin exchange (diffusion)

Polyimide-Polydimethylsiloxane

Small domains

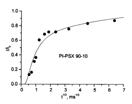

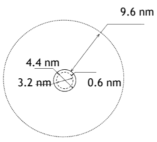

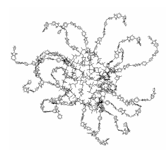

Size of dispersed component A in matrix B :

$$d_A = 2\frac{\varepsilon}{f_B}\left(\frac{1}{\pi}Dt_m^s\right)^{1/2}$$

Large domains

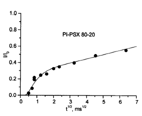

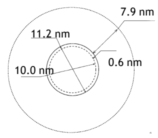

^1H-^1H WISE and off-resonance effect

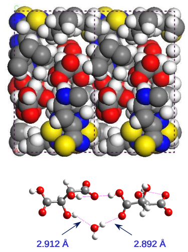

Location of external water molecules

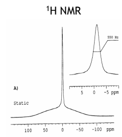

Weak dipolar interactions ^1H-^1H (1-2 kHz)
Narrow signal of H2O superimposed

Effect of ^1H chemical shif is not negligible (2-5 kHz)
Off-resonance detection = narraow dublet in the spectrum

2D ^1H-^{13}C WISE

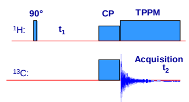

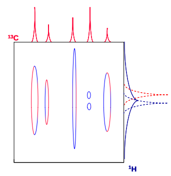

Location of external water molecules

Polysiloxane network

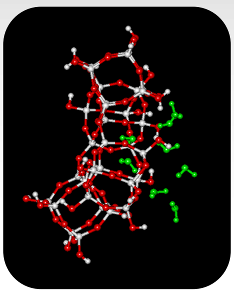

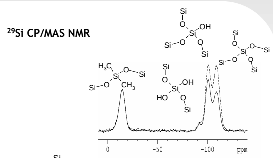

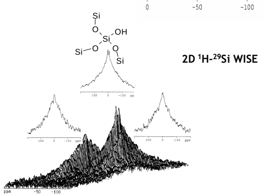

Location of external water molecules

Elastine-like polypeptide

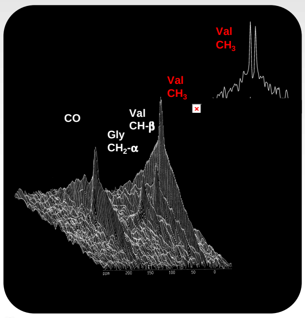

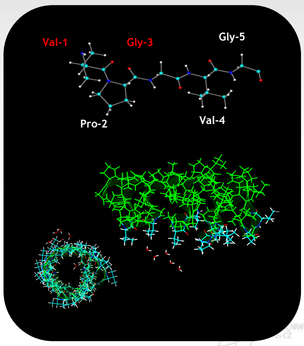

Dipolar couplings

Dipolar couplings and interatomic distances

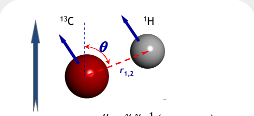

$$\hat{H}_D^{IS} = -\frac{\mu_0}{4\pi}\hbar\frac{\gamma_I\gamma_S}{r_{I,S}^3}\frac{1}{2}(3\cos^2\theta-1)2\hat{I}_z\hat{S}_z$$

Dipolar oscillation of ^{13}C NMR signal in a typical C-H group

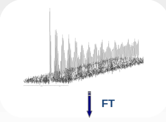

Dipolar spectrum of C-H group

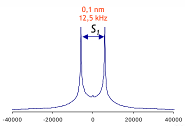

Scaling of D

$$r_{CH} = a\left(\frac{S_1}{2\pi}\right)^{-\frac{1}{3}}$$

$$S_1 = \sin\theta_m \frac{D_{IS}}{\sqrt{2}}$$

$$\sin\theta_m = 0.816$$

$$\theta_m = 54.7^\circ$$

- D - dipolar coupling constant depends on $1/r_{CH}^3$.
- D - dipolar coupling constant should be constant for all C-H pairs in CH or CH_2 groups as bond length is always ca. 0.11 nm

Dipolar couplings and segmental dynamics

Order parameter and motional models

Uniaxial rotational diffusion motion

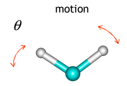

$$S_{CH} = 1-\frac{3}{2}\langle\theta^2\rangle$$

Dipolar spectrum

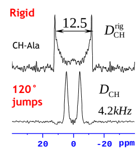

Order parametr

$$S_{CH} = \frac{D_{CH}}{D_{CH}^{rig}} = \frac{D_{CH}}{12.5(\text{kHz})}$$

Fast jumps

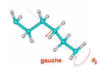

$$S_{CH}^2 = \sum_{i,j=1}^{N} p_i p_j P_2(\cos\theta_{ij})$$

Motion on the cone in parabolic potential

$$S^2 = 1-3\sin^2\theta\{\cos^2\theta(1-\exp[-\sigma_f^2]) + 0.25\sin^2\theta(1-\exp[-4\sigma_f^2])\}$$

Joint Laboratory of Solid-State NMR IMC AS CZ and IPMC AS CZ

Site-specific experiments

Simple measurement of dipolar couplings

Lee-Goldburg cross-polarization (LG-CP)

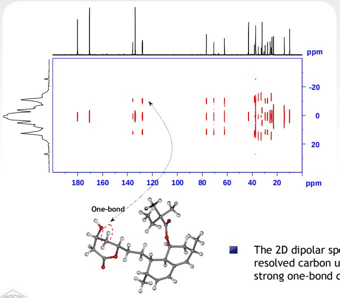

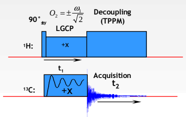

Hong, M. *et al. J. Phys. Chem. B* *106*, 7355 (2002).

- The 2D dipolar spectrum separates dipolar couplings for each resolved carbon unit. The obtained dipolar profiles are dominated by strong one-bond dipolar couplings.

Joint Laboratory of Solid-State NMR IMC AS CZ and IPMC AS CZ

Motional averaging and segmental dynamics

Fluctuation angle

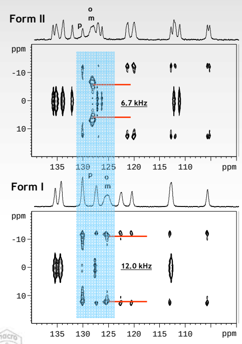

Metergoline

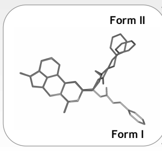

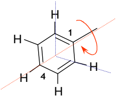

D = 6.7 kHz

$$S_{CH}^2 = \sum_{i,j=1}^{N} p_i p_j P_2(\cos\theta_{ij})$$

$$\theta_{ij} = 126^\circ$$

Fast jumps 180° along axis (1,4)

D = 12.0 kHz

$$\sigma = 16^\circ, \theta_0 = 60^\circ$$

$$S^2 = 1-3\sin^2\theta\{\cos^2\theta(1-\exp[-\sigma_f^2]) + 0.25\sin^2\theta(1-\exp[-4\sigma_f^2])\}$$

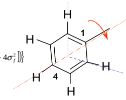

Dynamics in semicrystalline polymers

Standard Lee-Goldburg cross-polarization

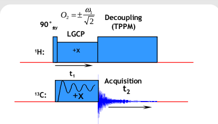

- Standard experiment is not "domain-selective" and dipolar profiles are detected both for mobile and rigid components.
- If NMR signals of both components are not resolved the resulting dipolar spectra must be considered as a superposition and combination of all contributions and motional modes.

Polyethylene (PE)

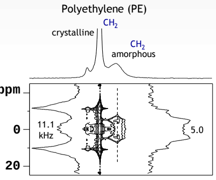

Polyamide-6 (PA-6)

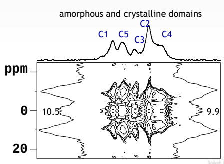

Joint Laboratory of Solid-State NMR IMC AS CZ and IPMC AS CZ

Selective detection of crystalline phase

T_1-filtered amplitude-modulated FSLG-CP experiment

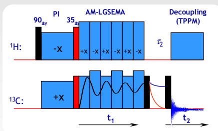

- **T_1-filtered amplitude-modulated** experiment detects data selectively from crystalline domains.
- **PA-6**: magnetization of amorphous component is suppressed; signals in both dimensions are narrowed. The measured dipolar couplings are not distorted.

Polyethylene (PE)

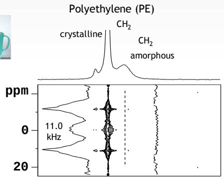

Polyamide-6 (PA-6)

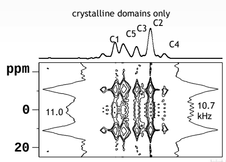

Joint Laboratory of Solid-State NMR IMC AS CZ and IPMC AS CZ

Selective detection of amorphous phase

Inverse-T_1-filtered amplitude-modulated FSLG-CP

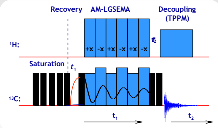

- **Inverse-T_1-filtered amplitude-modulated** FSLG-CP experiment back cross-polarization $^{13}C \rightarrow ^1H$ provides dipolar data selectively for amorphous domains.
- **PA-6**: magnetization of crystalline component is suppressed; signals in both dimensions are broadened due to conformational and motional heterogeneities.

Polyethylene (PE)

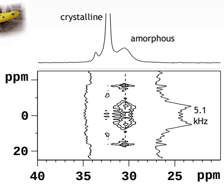

Polyamide - 6 (PA6)

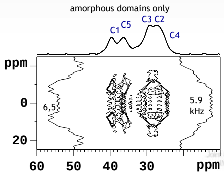

What about practical results?

Connection between molecular properties determined by ssNMR and macroscopic behavior

Spectral parameters and motional amplitudes

Macroscopic properties and mechanical behavior

Polymer/clay nanocomposites

Polyamide-6/MMT

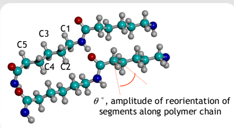

- Semicrystalline systems
- α-form, γ-form and amorphous phase
- Clay minerals cause
  - changes in composition
  - changes in T_g

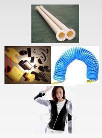

^{13}C CP/MAS NMR

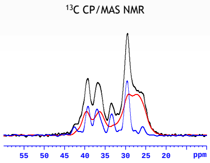

Loss modulus vs. temperature

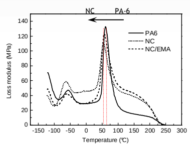

Semicrystalline polymers

Polyamide-6

T_1-filtered experiment

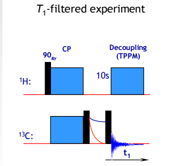

- Semicrystalline systems
- α-form, γ-form and amorphous phase
- Dynamics in both forms
- Domain-selective experiments
  - T_1-filtered experiment
  - Inverse-T_1-filtered experiment

Inverse-T_1-filtered experiment

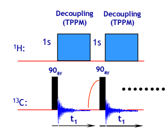

^{13}C CP/MAS NMR

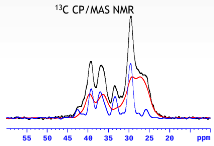

Crystalline phase

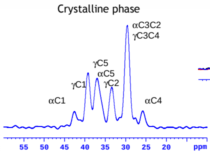

Amorphous phase

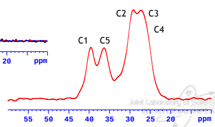

Semicrystalline polymers

Polyamide-6

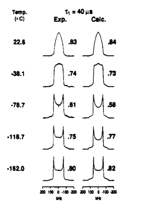

Miura, H.; Hirschinger, J.; English A.D. *Macromolecules*. 1990, 23, 2169.

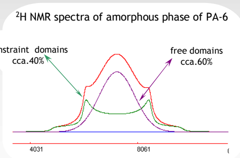

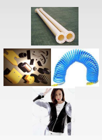

- Two components can be resolved in ^{2}H NMR spectra selectively measured for amorphous phase of PA-6
  - constraint chains
  - free chains

Amorphous phase

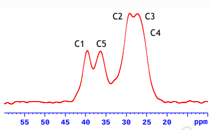

Segmental dynamics in polymer/clay nanocomposites

Domain-selective 2D FSLG-CP experiments

T_1-filtered experiment

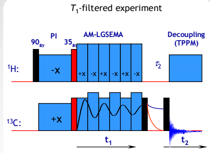

2D spectrum of crystalline phase

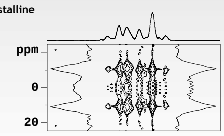

Inverse-T_1-filtered experiment

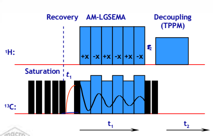

2D spectrum of amorphous phase

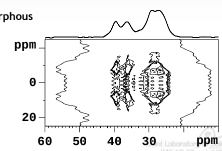

Brus J, Urbanova M, Kelnar I, Kotek J, *Macromolecules* 39 (16): 5400, (2006).

Motional amplitudes in polymer nanocomposites

Decrease in T_g in polymer nanocomposites

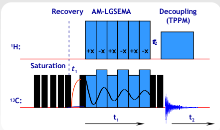

- **Nanocomposites** exhibits a bit surprising decrease in glass transition temperature.
- **Dipolar spectra** selectively measured for amorphous phase revealed **enhanced** motional amplitudes of some segments (C1) in nanocomposites.
- Fast and relatively low-amplitude wobbling occurring in glassy state can be considered as mechanically active

^{1}H-^{13}C dipolar profiles of amorphpous domains (C1)

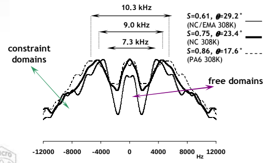

Temperature dependence of loss modulus

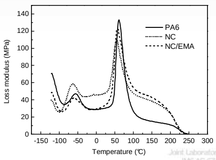

Brus J, Urbanova M, Kelnar I, Kotek J, *MACROMOLECULES* 39 (16): 5400, (2006).

BRUS J, URBANOVA M, STRACHOTA A, *MACROMOLECULES* 41 (2), 372-386 (2008).

Constraint and free polymer chains in PA-6/MMT systems

Inverse-T_1-filtered $T_{1\rho}$ relaxation experiments

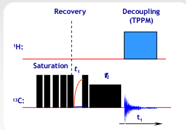

- **Amorphous phase in PA-6 nanocomposites** exhibits double-exponential (double-component) behavior.
- Inverse-T_1-filtered $T_{1\rho}$ relaxation is sensitive to high-amplitude mid-kilohertz frequency motions.
- **Fast component** - efficient relaxation in free domains due to trans-gauche jumps.

Relaxation profiles of various PA-6/MMT nanocomposites

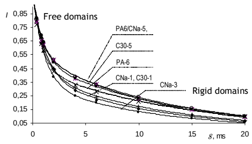

sample	$T_1(^{13}C)$	$T_{1\rho}(^{13}C)_a$	I_{slow}	$T_{1\rho}(^{13}C)_b$	I_{fast}
	(s)	(ms)	%	(ms)	%
PA6	1.15	12.8	45	0.8	55
PA6/CNa-1	0.98	11.0	36	1.2	64
PA6/CNa-3	0.93	10.8	34	1.1	66
PA6/CNa-5	0.95	11.0	57	0.8	43
PA6/C30-1	1.06	11.2	42	1.1	58
PA6/C30-3	1.09	12.0	55	0.9	45
PA6/C30-5	0.95	12.5	51	1.0	49

NMR parameters and mechanical properties

Fracture toughness and $T_{1\rho}$ relaxation

Mechanical properties

Fracture toughness as a function of clay content

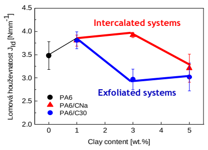

NMR spin properties

Intensity of rapidly relaxing component as a function of clay content

relative amounts of free domains in amorphous phase of PA-6

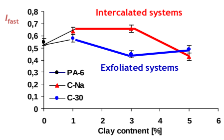

Summary

Wide Line Separation - WISE

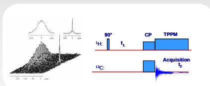

Size of domains in heterogenous systems

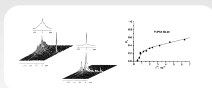

Location of external water

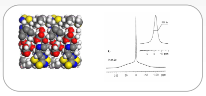

Solid-state NMR and ...

Spin diffusion

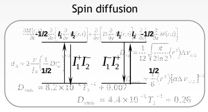

Segmental dynamics in semicrystalline systems

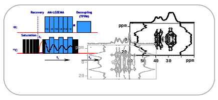

Order parameter and fluctuation angle